

Spectroscopic investigation of trinuclear metallic cluster encapsulated in silico 9- wolframic heteropolyanion

M. HOSSU, A. ILIE^a, D. RUSU^b, O. COZAR, M. RUSU^a, L. DAVID^{*}

^a"Babes-Bolyai" University, Faculty of Chemistry, 400028, Cluj Napoca, Romania

^a"Babes-Bolyai" University, Faculty of Physics, 400084 Cluj-Napoca, Romania

^b"Iuliu Hatieganu" University Faculty of Pharmacy, 400032 Cluj-Napoca, Romania

The polyoxometalate $[M_3^{n+}(H_2O)_6(SiW_9O_{34})_2]^{(20-3n)-}$, $M = Fe(III)$ (1), $Co(II)$ (2), $Ni(II)$ (3) was prepared and investigated by thermal analysis, FTIR, UV-Vis and ESR spectroscopies in order to determine the coordination of metallic ions, the local symmetry around them and the spin state. The co-ordination mode of transition metal ions was made by means comparison between the FTIR spectra of the sandwich-type complexes with those of α -A- $Na_{10}[SiW_9O_{34}] \cdot 24H_2O$ ligand. The relatively small shift of the $\nu_{as}(W=O_t)$ vibration band is due to the fact the terminal O_t atoms are not involved in the metal ions co-ordination. The opposite shift of $\nu_{as}(W-O_e-W)$ and $\nu_{as}(W-O_c-W)$ frequencies for the bonding from the belt region shows the co-ordination of each metallic ion at oxygen atoms from corner-sharing octahedral. The UV electronic spectra of the sandwich-type complex and of the ligand contain two bands characteristic for the ligand to metal charge transfer in the heteropolyoxometalates frame. Information about the local environment of $Fe(III)$, $Co(II)$ and $Ni(II)$ ions have been obtained by means of d-d transitions from the visible electronic spectrum performed in aqueous solution. Powder ESR data show the presence of small antiferromagnetic interactions in the spin frustrated trinuclear metallic clusters.

(Received November 15, 2006; accepted December 21, 2006)

Keywords: Trinuclear metallic cluster, FTIR, ESR

1. Introduction

During the last years, interest for heteropolyoxometalates (HPOM) substituted by early transition metals (3d) has been continuously growing [1-3]. These complexes have the capacity to include more transition metals, which interact by means of dipolar or exchange coupling [4, 5]. This aspect recommends heteropolyoxometalates as potential hosts of high dimensional clusters [4]. Heteropolyoxometalates have also received much attention because of the vast range of applications, in material science, medicine, catalysis [3, 6]. Heteroatoms Si^{IV} are tetrahedrally coordinated by oxygen atoms in these fragments and the fourth oxygen acting toward the lacunary region is involved in coordination to the metallic cluster. A special class of heteropolyoxometalates is the unsaturated trilacunary Keggin-type $[X^{n+}W_9O_{33}]^{(12-n)-}$ structure, where the heteroatom X is the Si^{IV} ion [7-9]. The main characteristic of this ion is the presence of one pair of electrons, which prevents further condensation to a saturated Keggin structure [7]. However, transition metal ions could link the lacunary units, resulting a sandwich-type structure. Our interest was focused on structures with two trivacant Keggin fragments linked by a trinuclear cluster of $Fe(III)$ (1), $Co(II)$ (2), $Ni(II)$ (3) ions (Fig. 1).

In this paper we report the synthesis and physical properties of the new series of sodium salts of the sandwich-type $[M_3^{n+}(H_2O)_6(SiW_9O_{34})_2]^{(20-3n)-}$ ($M = Fe(III)$ (1), $Co(II)$ (2), $Ni(II)$ (3)) heteropolyanion (Fig. 1). In order to obtain information about the coordination of

the metallic ions to the trivacant ligand, their oxidation state and the local symmetry around them, the FTIR and UV-VIS measurements were performed. Precious information on the spin state of the metallic cluster and the type of metal-metal coupling was provided by the EPR spectra.

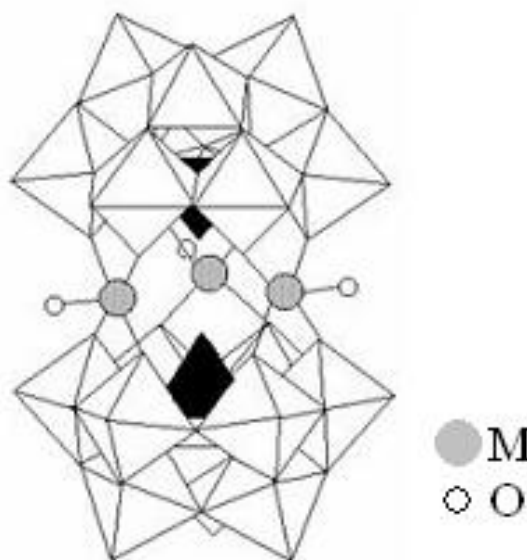


Fig. 1. The structure of the $[M_3^{n+}(H_2O)_6(SiW_9O_{34})_2]^{(20-3n)-}$ heteropolyanion. (The empty polyhedra are WO_6 units and the full trigonal pyramids are SiO_4).

2. Experimental section

All chemicals were of reagent grade and used as received. $\text{Na}_{10}[\text{SiW}_9\text{O}_{34}] \cdot 24\text{H}_2\text{O}$ have been synthesized as previously described [10].

The $\text{Na}_{10}[\text{SiW}_9\text{O}_{34}] \cdot 24\text{H}_2\text{O}$ ligand was prepared according to the method described by Hervé.

Synthesis of $\text{Na}_{11}[\text{Fe}_3(\text{H}_2\text{O})_6(\text{SiW}_9\text{O}_{34})_2] \cdot 25\text{H}_2\text{O}$ complex (1)

5.75 g (2 mmol) $\text{Na}_{10}[\text{SiW}_9\text{O}_{34}] \cdot 24\text{H}_2\text{O}$ was dissolved in 15 ml of distilled water. Next 0.8 g (3 mmol) $\text{FeCl}_3 \cdot 6\text{H}_2\text{O}$ was dissolved in 10 ml of distilled water was slowly added at 50°C while stirring, the mixture was subsequently stirred for 15 min. The resulting yellow-orange solution was filtered through a medium frit and allowed to cool to room temperature. The precipitation was obtained by filtration and washed with water distilled (5°C), which was recrystallized, from a minimum amount of hot water (15 ml). After 3-4 days crystals were collected Yield: 2.97, (55%).

Synthesis of $\text{Na}_{14}[\text{Co}_3(\text{H}_2\text{O})_6(\text{SiW}_9\text{O}_{34})_2] \cdot 45\text{H}_2\text{O}$ complex (2)

5.75 g (2 mmol) $\text{Na}_{10}[\text{SiW}_9\text{O}_{34}] \cdot 24\text{H}_2\text{O}$ was dissolved in 15 ml of distilled water. Next 0.3 g (3 mmol) $\text{CoCl}_2 \cdot 2\text{H}_2\text{O}$ was dissolved in 10 ml of distilled water were added while stirring, the mixture was subsequently stirred for 15 min. The resulting solution was filtered and allowed to result in immediate precipitation of a yellow - orange product, which was recrystallized, from a minimum

amount of hot water (15 ml). After 3-4 days crystals were collected Yield: 4.44, (76%).

Synthesis of $\text{Na}_{14}[\text{Ni}_3(\text{H}_2\text{O})_6(\text{SiW}_9\text{O}_{34})_2] \cdot 25\text{H}_2\text{O}$ complex (3)

5.75 g (2 mmol) $\text{Na}_{10}[\text{SiW}_9\text{O}_{34}] \cdot 24\text{H}_2\text{O}$ was dissolved in 15 ml of distilled water. Next 0.53 g (3 mmol) $\text{NiCl}_2 \cdot 6\text{H}_2\text{O}$ was dissolved in 10 ml of distilled water were added while stirring, the mixture was subsequently stirred for 15 min. The resulting solution was filtered and allowed to result in immediate precipitation of a yellow - orange product, which was recrystallized, from a minimum amount of hot water (15 ml). After 3-4 days crystals were collected Yield: 3.56, (65%).

3. Results and discussion

3.1 Chemical analysis

The composition in of Fe, Co, Ni, W and Si each complex was determined by atomic absorption (Table 1). The water content was estimated on the basis of thermal analysis performed using a Paulik Erdely OD-102 derivatograph. Thermogravimetric studies were carried out on 0.4608 g $\text{Na}_{11}[\text{Fe}_3(\text{H}_2\text{O})_6(\text{SiW}_9\text{O}_{34})_2] \cdot 25\text{H}_2\text{O}$, 0.3760 g $\text{Na}_{14}[\text{Co}_3(\text{H}_2\text{O})_6(\text{SiW}_9\text{O}_{34})_2] \cdot 45\text{H}_2\text{O}$ and 1.1872 g $\text{Na}_{14}[\text{Ni}_3(\text{H}_2\text{O})_6(\text{SiW}_9\text{O}_{34})_2] \cdot 25\text{H}_2\text{O}$ 20 mg samples at a heating rate of $10^\circ\text{C min}^{-1}$. The TG curves exhibited a step below 20°C , which corresponds to the loss of lattice water (endothermic). Above 800°C , the inorganic residue exhibits some minor exothermic effect, probably due to a polymorphic transformation of the metal oxides mixture.

Table 1. Analytical data of the synthesized compounds.

Compound	Na %		Si %		W%		M %		H ₂ O %	
	Calcd.	Found	Calcd.	Found	Calcd.	Found	Calcd.	Found	Calcd.	Found
1	4.65	4.45	1.30	1.33	60.92	59.20	3.08	3.12	10.27	1.034
2	5.48	5.42	0.95	0.91	63.04	62.94	3.01	3.04	15.64	15.72
3	5.84	5.76	1.01	0.98	60.06	60.02	3.26	3.30	10.12	10.15

3.2 FT-IR spectra

FT-IR spectra were recorded on a Jasco FT/IR 610 spectrophotometer in the $4000\text{--}400\text{ cm}^{-1}$ range, using KBr pellets [11].

Some information about of the Fe (III), Co (II) and Ni (II) ions to the trivacant Keggin units, about the local symmetry and the bonds strength were obtained by comparing the FT-IR spectra of the metallic compounds and those of corresponding ligand $\text{Na}_{10}[\text{SiW}_9\text{O}_{34}] \cdot 24\text{H}_2\text{O}$.

Some characteristic frequencies are summarized in Table 2 and the main region of FT-IR spectra are given in Fig. 2.

The band due to the stretching frequency of the $\nu_{\text{as}}(\text{W}-\text{O}_t)$ bond is shifted toward higher frequencies with 3 cm^{-1} (1) and 1 cm^{-1} (2) which indicates the non-participation of the terminal atoms of oxygen to the coordination at metallic ions, as well as the stability of the polyoxowolframic trilacunar fragments.

The bands due to the $\nu_{\text{as}}(\text{Si}-\text{O}_a)$ and $\nu_{\text{as}}(\text{W}-\text{O}_c-\text{W})$ stretching vibrations are superposed and are shifted with

15 cm^{-1} for the complex (**1**), with 1 cm^{-1} for (**2**) with 3 cm^{-1} for (**3**) and towards higher frequencies given the ligand.

In the Fe complex, the band $\nu_{\text{as}}(\text{W}-\text{O}_e-\text{W})$ due to the stretching vibration of the tricentric bonds is split into two components both for the complex and ligand as a consequence of the participation of oxygen O_e atoms at the coordination of Fe (III) ions.

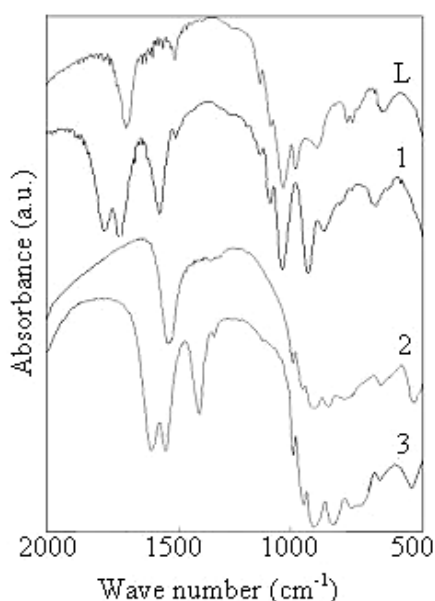


Fig. 2. FTIR spectra of the ligand **L** and the sandwich-type complexes: **1**, **2** and **3**.

3.3 Electronic spectroscopy

The electronic spectra evidenciate the characteristic of the complex combinations of polyoxometalates in which

the Keggin anion plays the role of the ligand and the secondary heteroatoms are cations of the transitional metals.

The UV electronic spectra of the sandwich-type complex and of the ligand contain two bands characteristic for the ligand to metal charge transfer in the heteropolyoxometalates frame. The more intense band corresponding to the $p_{\pi}(\text{O}_t) \rightarrow d_{\pi^*}(\text{W})$ [13] itions is centred at 46290 cm^{-1} for (**L**), 46569 cm^{-1} for (**1**), 46680 cm^{-1} for (**2**) and 46626 cm^{-1} for (**3**). This is in agreement with the coordination of the Fe (III), Co (II) and Ni (II) ions in the lacunary region of the ligand and not to the terminal oxygen atoms. The broader band centred at 38461 cm^{-1} in the ligand spectrum belongs to the $p_{\pi}(\text{O}_{c,e}) \rightarrow d_{\pi^*}(\text{W})$ change transfer transition in the tricentric bonds[14]is absorption band appears at 38910 cm^{-1} , 40485 cm^{-1} and 39215 cm^{-1} in the UV spectra of the Fe (III), Co (II) and respectively Ni (II) complexes (Fig. 3).

Information about the local environment of 3d metal ions in the complex **1-3** have been obtained by means of d-d transitions from the visible electronic spectrum performed in aqueous solution (Fig. 4).

The VIS spectrum of complex **1** contains an $\text{Fe}^{\text{III}} \leftarrow \text{O}$ charge transfer band starting at about 20000 cm^{-1} and a shoulder at $\approx 21000 \text{ cm}^{-1}$ (Fig. 4) [15].

Table 2. FT-IR data (cm^{-1}) for the ligand **L**, **1**, **2** and **3** complexes^a.

Bands	L	1	2	3
$\nu_{\text{as}}(\text{Si}-\text{O}-\text{Si})$	1141 w, 1100 w	1163 w, 1111 w	1128 w, 1058 w	1154 w, 1128 w
$\nu_{\text{as}}(\text{W}=\text{O}_t)$	987 m	990 m	988 m	987 m
$\nu_{\text{as}}(\text{Si}-\text{O}_a)$	937 s	952 s	938 s	940 s
$\nu_{\text{as}}(\text{W}-\text{O}_c-\text{W})$	878 vs, 844 vs	903 vs	880 vs	893 vs
$\nu_{\text{as}}(\text{W}-\text{O}_e-\text{W})$	810 vs, 723 vs	797 vs, 733 vs	805 vs, 720 vs	807 vs, 722 s
$\delta(\text{W}-\text{O}_{c,e}-\text{W})$	618 s	669 m	659 w	682 s

^a w, weak; m, medium; s, strong; vs, very strong; sh, shoulder;

O_a is the oxygen which links the Si and W atoms, $\text{O}_{c,e}$ connect corner and edge-sharing octahedra, respectively, O_t is a terminal oxygen.

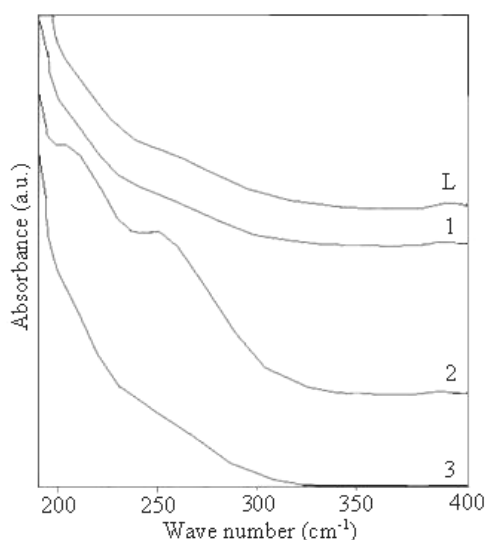


Fig. 3. The UV spectra of the ligand **L** and complexes.

Complex **2** has very weak absorption in the 10000–24000 cm^{-1} region of the VIS spectrum and a charge transfer band at more than 28000 cm^{-1} (Fig. 5). Two bands centered at $\approx 18455 \text{ cm}^{-1}$ and $\approx 20880 \text{ cm}^{-1}$ appear by increasing the coordination of the studied solution. These have been assigned to the ${}^4\text{E}({}^4\text{T}_1) \rightarrow {}^4\text{E}({}^4\text{T}_1(\text{P}))$ and ${}^4\text{E}({}^4\text{T}_1) \rightarrow {}^4\text{A}_2({}^4\text{T}_1(\text{P}))$ transition respectively, for high-spin Co (II) ions in a square pyramidal environment. There is an attempt to form a new band at $\approx 13000 \text{ cm}^{-1}$, but it is very low and nearly obscured by the baseline [16].

The VIS spectrum of complex **3** (Fig. 6) shows a broad band in the at 10000–18000 cm^{-1} region and a charge transfer band above at $\approx 20000 \text{ cm}^{-1}$. The three absorption bands centered at 13020, 14685 and 16114 cm^{-1} obtained by a Gaussian analysis are in the range typical for five – coordinated high-spin Ni (II) ions with a C_{2v} local symmetry. The corresponding transitions are ${}^3\text{B}_1 \rightarrow {}^3\text{B}_1({}^3\text{T}_1)$, ${}^3\text{B}_1 \rightarrow {}^3\text{A}_2({}^3\text{T}_1)$ and ${}^3\text{B}_1 \rightarrow {}^1\text{A}_1({}^1\text{D})$, respectively [17].

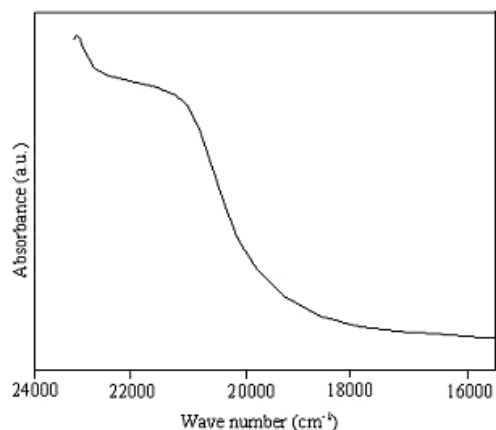


Fig. 4 The visible electronic spectrum of the complex **1** in $5 \times 10^{-3} \text{ mol l}^{-1}$ aqueous solution.

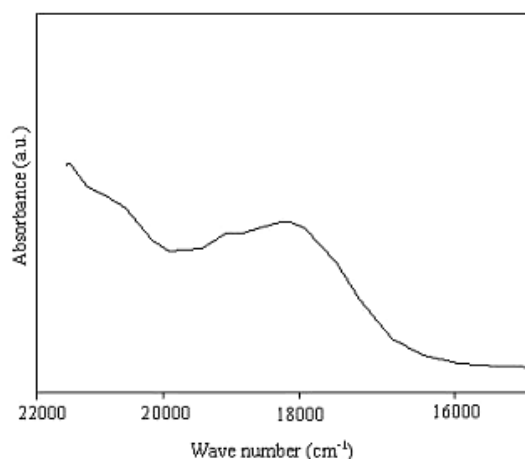


Fig. 5 The visible electronic spectrum of the complex **2** in $5 \times 10^{-3} \text{ mol l}^{-1}$ aqueous solution.

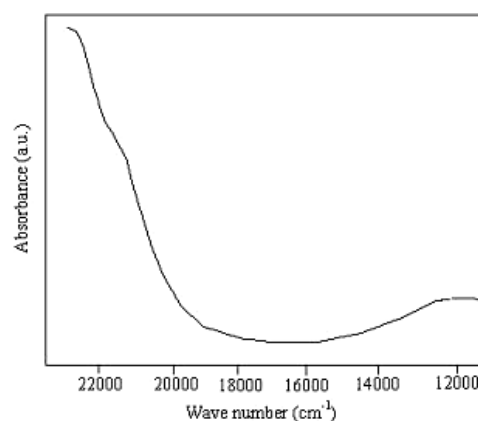


Fig. 6. The visible electronic spectrum of the complex **3** in aqueous solution.

3.4. EPR spectra

The powder ESR spectrum obtained in the X-band at $T = 80 \text{ K}$ for the complex **1** contains three main features at the effective g values 8.493, 4.289 and 2.000 and a shoulder at 5.498. The g value greater than 6.0 indicates that at this temperature the complex is characterized by one $S \geq 5/2$ spin state (Fig. 7).

The powder ESR spectrum of the complex **2**, recorded in the X-band (9.7 GHz) at $T = 80 \text{ K}$, exhibits a very broad signal ($\Delta B(\text{p-p}) \approx 2160 \text{ G}$) centered at $g = 3.582$ and a small signal at $g \approx 2.0$. Only the last signal remains in the spectrum when increasing the temperature. The observation of this signal even at room temperature is in good agreement with the presence of coupled Co (II) ions, with square pyramidal local environments.

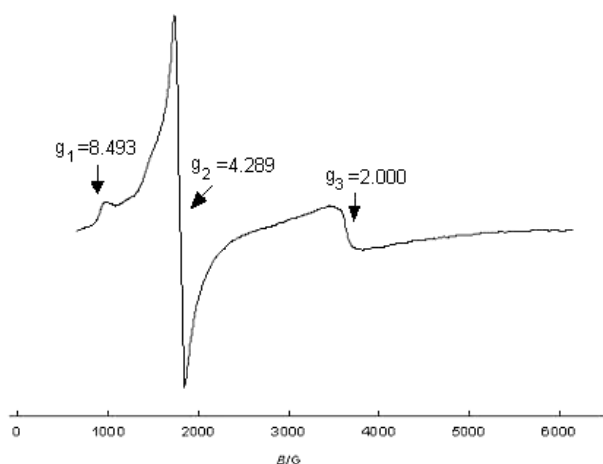


Fig. 7. The powder ESR spectrum of the complex 1 at $T = 80$ K.

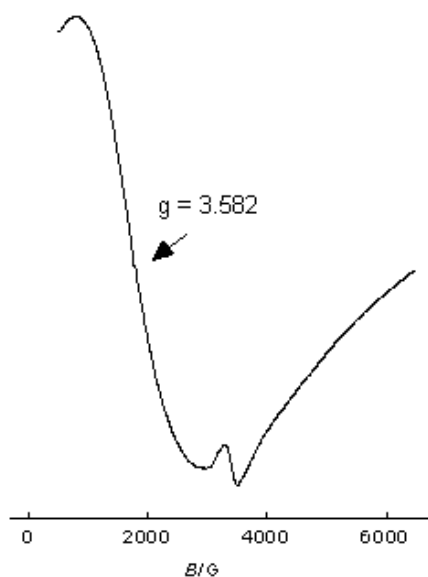


Fig. 8. The powder ESR spectrum of the complex 2 at $T = 80$ K.

4. Conclusions

Spectroscopic investigations of the sodium salts of the $[M_3^{n+}(H_2O)_6(SiW_9O_{34})_2]^{(20-3n)-}$ heteropolyanions confirm the sandwich-type structure of these complexes and the encapsulation of the trinuclear metal cluster between two trivacant Keggin units.

FTIR data indicate the coordination of each metallic ion to oxygen atoms from the corner-sharing octahedra.

The charge transfer into the terminal $W=O_t$ bonds is unaffected by the metal ions. The coordinations of the Fe (III) ions to the trivacant ligand decrease the energy for the charge transfer into the HPOM cage. The LMCT bands ($M \rightarrow O$) in the VIS spectra are direct proof of the existence of metal-oxygen bonding. Transition metal ions are penta-coordinated in square-pyramidal environment and the local symmetry is C_{4v} (Co (II)) or C_{2v} (Ni (II)). The ions with more 3d electrons are in a high-spin state.

References

- [1] D.E. Katsoulis, *Chem. Rev.* **98**, 359 (1998).
- [2] M. T. Pope, *Heteropoly and Isopoly Oxometalates*, Springer-Verlag, Berlin (1983).
- [3] X. Zhang, Q. Chen, D.C. Duncan, C. F. Campana, C. L. Hill, *Inorg. Chem.* **36**, 4208 (1997).
- [4] A. Müller, F. Peters, M. T. Pope, D. Gatteschi, *Chem. Rev.* **98**, 239 (1998).
- [5] C. J. Gómez-García, E. Coronado, P. Gómez-Romero, N. Casañ-Pastor, *Inorg. Chem.*, **32**, 89 (1993).
- [6] N. Mizuno, M. Misono, *Chem. Rev.* **98**, 199 (1998).
- [7] I. Loose, E. Drost, M. Bösing, H. Pohlmann, M. H. Dickman, C. Rosu, M. T. Pope, B. Krebs, *Inorg. Chem.* **38**, 2688 (1999).
- [8] C. Tourné, A. Revel, G. Tourné, M. Vendrell, C. R. Acad. Sci. Paris C277, (1973), p. 643.
- [9] A. Mazeud, N. Ammari, F. Robert, R. Thouvenot, *Angew. Chem.*, **35**, 1961, (1996).
- [10] B. Krebs, R. Klein, in *Polyoxometalates: From Platonic Solids to Anti-Retroviral Activity*, M. T. Pope and A. Müller (Eds.), Kluwer Publishers, Dordrecht, 1994.
- [11] Knoth, W. H., Domaille, P. J. L., Harlow, R. L., *Inorg. Chem.*, **25**, 1577, (1986).
- [12] G. Hervé, A. Tézé, *J. Inorg. Nucl. Chem.*, **39**, 2151 (1977).
- [13] T. Yamase, *Chem. Rev.* **98**, 307 (1998).
- [14] H. So, M. T. Pope, *Inorg. Chem.*, **23**, 3292, (1984).
- [15] E. Cadot, M. Fournier, G. Hervé, A. Tézé, *Inorg. Chem.* **35**, 282 (1996).
- [16] U. Kortz, S. Isber, M. H. Dickman, D. Ravot, *Inorg. Chem.* **39**, 2915 (2000).
- [17] A. B. P. Lever, "Inorganic Electronic Spectroscopy", Elsevier, New York, 2nd edn., 1984, (a) p. 452, (b) p. 507.

*Corresponding author: leodavid@phys.ubbcluj.ro